Lung Sound Classification Using Wavelet Transform and Entropy to Detect Lung Abnormality

Achmad Rizal[1], Attika Puspitasari[1]

Abstract: Lung sounds provide essential information about the health of the lungs and respiratory tract. They have unique and distinguishable patterns associated with the abnormalities in these organs. Many studies attempted to develop various methods to classify lung sounds automatically. Wavelet transform is one of the approaches widely utilized for physiological signal analysis. Commonly, wavelet in feature extraction is used to break down the lung sounds into several sub-bands before calculating some parameters. This study used five lung sound classes obtained from various sources. Furthermore, the wavelet analysis process was carried out using Discrete Wavelet Transform (DWT) and Wavelet Package Decomposition (WPD) analysis and entropy calculation as feature extraction. In the DWT process, the highest accuracy obtained was 97.98% using Permutation Entropy (PE), Renyi Entropy (RE), and Spectral Entropy (SEN). In WPD, the best accuracy achieved is 98.99 % when 8 sub-bands and RE are used. These results are relatively competitive compared with previous studies using the wavelet method with the same datasets.

Keywords: Wavelet transform, Sub-bands, Entropy, Feature reduction, Classifier.

1   Introduction

Lung sounds contain necessary information about the health of the lungs and respiratory tract. They have unique and distinguishable patterns associated with the abnormalities that probably occurred [1]. Therefore, many studies attempted to develop various methods to classify lung sounds automatically. Wavelet transform is one of the methods frequently used for physiological signals analysis [2]. Commonly, wavelet in feature extraction is used to break down the lung sounds into several sub-bands before calculating some parameters [3].

Certain studies have been carried out to classify lung sounds using wavelet analysis. Kandaswamy et al., for instance, used the 7th level of Discrete Wavelet Transform (DWT) to decompose the lung sound signals [4] with the

---

[1]School of Electrical Engineering, Telkom University, Indonesia;
 E-mails: achmadrizal@telkomuniversity.ac.id; attikapuspitasari@yahoo.com

characteristics of mean absolute value, mean average power, standard deviation of coefficient, and ratio of mean absolute value of the adjacent sub-band. Hashemi et al. used skewness and kurtosis for feature extraction in the signal sub-bands [5]. Wavelet Packet Decomposition (WPD) is another approach that decomposes the detailed and approximation sub-bands of the analysis process. Rizal et al. used the WPD level to classify lung sounds using the specific sub-band selection scenario [6]. Ref. [2] shows a comparison of the performance of WPD and DWT for lung sound categorization, with DWT producing greater accuracy but employing more features.

One of the features used in previous studies is entropy, a metric for assessing the randomness of the signals [7]. Shannon entropy was combined with various features as the extraction method in the sub-bands of wavelet analysis. However, the measurement of wavelet and entropy transformation in lung sound classification has not been conducted. Therefore, only Shannon entropy was used for feature extraction in the wavelet sub-bands.

This study proposes the combination of WPD/DWT with various entropies for feature extraction. The WPD and DWT schemes in [4] and [6] were combined with Shannon, Spectral, Renyi, Wavelet, Approximate, Sample, Permutation, and Tsalli entropy. Furthermore, the sub-bands selection process was carried out and resulted in the highest accuracy. Multilayer Perceptron (MLP) was used as the classifier in which the results were compared with previous studies [2]. This study is expected to obtain the recommendations for the best entropy method for lung sound classification using wavelet analysis.

2 Study Methods

2.1 Lung Sounds Datasets

Table 1 shows the lung sound data used in which 99 data were obtained from various sources such as from CD complimentary books [8], the internet as in [9], and [10]. The resources provide multiple classes representing several normal and abnormal lung sound cases. As a result, the sounds with the most data reflected numerous aspects of lung sounds, such as Continuous Adventitious Sounds (CAS) and Discontinuous Adventitious Sounds (DAS). The classes were obtained using the data presented in **Table 1**, which included normal sound from bronchial data, wheeze, crackle, pleural rub, and stridor data classes. Each lung sound data consists of one respiration cycle, one inspiration, and one expiration, with a sample length of $15000-34000$ and a sampling frequency of 8000 Hz.

Normal sounds are non-musical and heard in the inspiratory and expiratory phases, indicating a healthy lung condition [11]. There are four normal lung sounds based on location: normal tracheal, normal bronchial, normal bronchovesicular, and normal vesicular sound [11]. The normal bronchial sound was used as the dataset in this study. Fig. 1 depicts the signal plot and frequency

spectrum of normal lung sounds. There is a distinct difference between the expiration and inspiration stages. The signal energy tends to be uniform at a frequency below 1000 Hz. Meanwhile, crackle is an adventitious non-musical respiratory sound that is short, explosive, and classified into fine and coarse [12]. Fig. 2 illustrates the signal plot and spectrum of this type of sound, with signal energy that tends to be a frequency below 300 Hz. The crackle sound indicates several signal pulses in the signal plot, and some of the diseases that produce this sound are asbestosis and pneumonia. Furthermore, wheeze is a high-pitched, continuous musical lung sound heard during inspiration, expiration, or both phases [11]. Asthma is one of the lung diseases that causes wheezing. Figure 3 describes the signal plot and spectrum of wheeze sound, and the dominant frequency appears around $300-400$ Hz, which is indicated by a sharp increase in the signal spectrum. A pleural or friction rub is the lung sound associated with pleural inflammation or tumor [11]. Meanwhile, stridor is a low-frequency wheeze sound that is common with tracheal stenosis [8]. In the inspiration phase, the stridor has a wheeze-like pattern with the lower pitch. Class-imbalance does not occur despite the differences in the amount of data since the percentage difference in amounts is small.

Table 1
Lung Sounds Data.

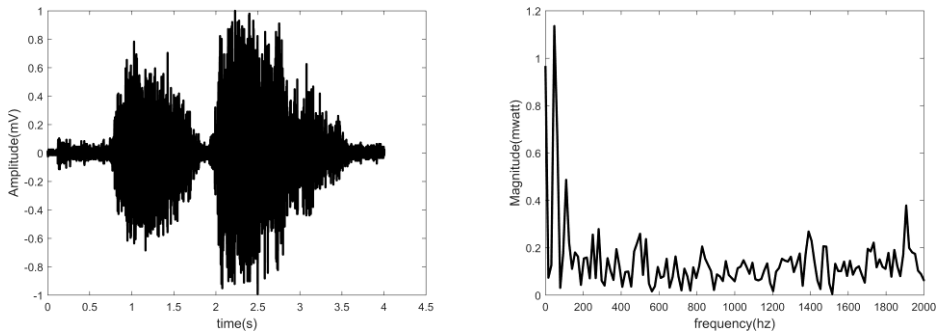| Data Classes	Amount of Data	Percentage
Normal bronchial	22	22,22%
Crackle	21	21,21%
Wheeze	18	18,18%
Friction rub	18	18,18%
Stridor	20	20,20%

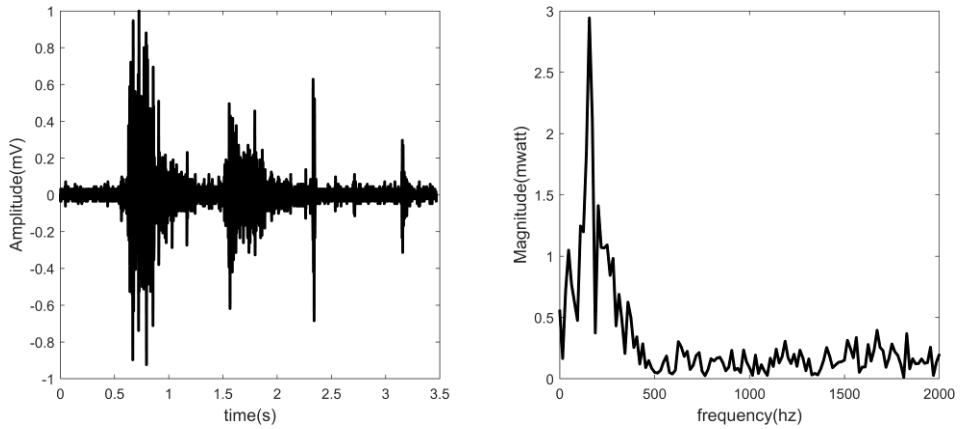**Fig. 1** − *Normal Lung Sound and the Frequency Spectrum.*

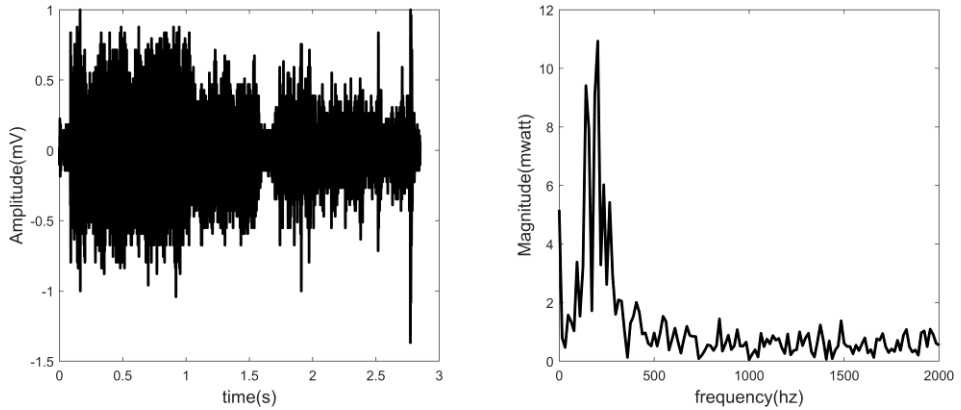**Fig. 2** − *Crackle Sound and the Frequency Spectrum.*

Fig. 3 − *Wheeze Sound and the Frequency Spectrum.*

2.2 Wavelet transform

Multiresolution analysis is always associated with wavelet analysis. One of the advantages of wavelet analysis over other methods is the simplicity with which the signal resolution may be varied in response to the frequency bandwidth [4]. Mathematically, the wavelet transform can be shown in (1) [13]:

$$WT_x^{\psi}\left(\tau, s\right) = \frac{1}{\sqrt{|s|}} \int x(t)\psi^{*}\left(\frac{t-\tau}{s}\right) \mathrm{d}t \ . \tag{1}$$

The variable *s*, τ and ψ(*t*) represents scale, dilation, and mother wavelet. The choice of dilation and scale changes the observed signal resolution. Meanwhile, the mother wavelet used includes Haar, Daubechies2 (DB2), Daubechies8 (DB8), Biorthogonal1.5 (Bior1.5), and Biorthogonal2.8 (Bior2.8). The selection was

based on previous studies' best results [14], and the calculation of signal complexity was conducted on the wavelet sub-bands. The sub-bands based on the decomposition included Discrete Wavelet Transform (DWT) and Wavelet Packet Decomposition (WPD). Furthermore, the scheme of each decomposition is described below.

2.2.1 Discrete Wavelet Transform (DWT)

In DWT, the input signal $x(t)$ was put into a pair of LPF and HPF filters before being downsampled. The output of the HPF was called the detail components, while LPF was called the approximation components. This approximation component is decomposed at the following level. The DWT process is shown in Fig. 4.
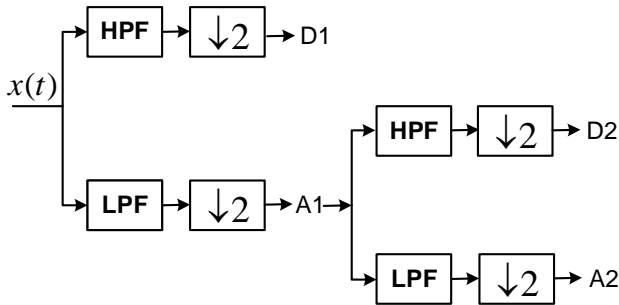

Fig. 4 – *Scheme of 2nd Level of DWT.*

The 7th level of DWT was used in this study, resulting in 8 sub-bands for each bandwidth, as indicated in **Table 2**, as conducted by Kandaswamy et al. [4] and Hasheemi et al. [5].

Table 2
Frequencies Range for Each Sub-bands in Wavelet Decomposition.

Sub-band	$f_s = 8000$ Hz
D1	2000 – 4000
D2	1000 – 2000
D3	500 – 1000
D4	250 – 500
D5	125 – 250
D6	62,5 – 125
D7	31,25 – 62,5
A7	0 – 31,25

2.2.2 Wavelet Packet Decomposition (WPD)

In DWT, only the approximate components were decomposed, while in WPD, all components were decomposed. Furthermore, 2N sub-bands are obtained when WPD is set to N, as shown in Fig. 5.
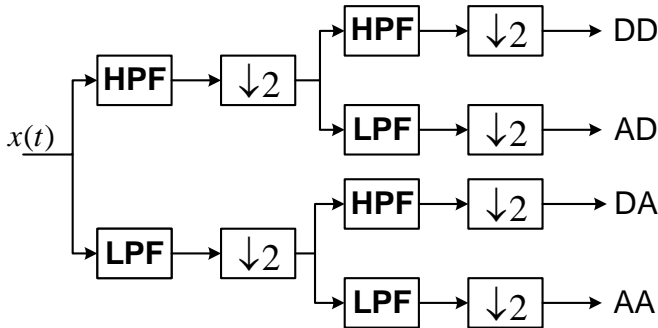

Fig. 5 – *The 2ⁿᵈ Level of WPD.*

In this study, the decomposition was conducted up to the 5th level, and only 15 sub-bands were used to calculate the characteristics of lung sounds [6]. The frequencies range of each sub-bands for each f_s = 8000 Hz is shown in **Table 3**.

Table 3
Frequencies Range for Each Sub-bands Used in WPD.

Frequency range (Hz)	Lung sound's sub-band				
0 - 250	A1	AA2	AAA3	AAAA4	AAAAA5
					DAAAA5
250 - 500				DAAA4	ADAAA5
					DDAAA5
500 - 1000			DAA3	ADAA4	AADAA5
					DDDAA5
				DDAA4	ADDAA5
					DDDAA5
1000 -2000		DA2	*ADA3*	*AADA4*	
				DADA4	
			DDA3	*ADDA4*	
				DDDA4	
2000 - 3000	*D1*	*AD2*	*AAD3*		
			DAD3		
3000 - 4000		*DD2*			

2.3 Entropy

The second approach used the system's entropy to compute the signal complexity. Meanwhile, statistics were used to determine how regular and complicated signals were, while entropy was used as a feature of the statistical analysis in the previous technique. This study used several entropy calculation techniques.

2.3.1 Shannon entropy

Shannon Entropy (ShEN) is the measurement of signal complexity [15]. Mathematically, it is shown in (2).

$$ShEN = -\sum_{i=1}^{N} p_i \log_2 p_i , \tag{2}$$

where p_i is the probability of the sample value in the signal $x(i)$. Generally, the signal histogram is employed to aid in the calculation of *ShEN*.

2.3.2 Spectral entropy

Spectral Entropy (SEN) is the normalized form of *ShEN* calculated from the signal spectral, which describes the signal spectrum's irregularity. It is shown in (3).

$$SEN = -\sum_{f=0}^{fh} p_f \log_2 \left(\frac{1}{p_f} \right), \tag{3}$$

where p_f represents the power density of the frequency band, and f_i and f_h represent the boundary frequency of the signal. The signal's power is normalized, hence, $\sum p_n = 1$ [15].

2.3.3 Renyi entropy

Renyi Entropy (RE) is the common form of entropy calculation [16]. Mathematically, it can be expressed as in (4).

$$S_q = \frac{1}{1-q} \log_2 \left(\sum_{i=1}^{N} p_i^q \right), \quad q \neq 1. \tag{4}$$

Practically, RE is only used for $q = 2$.

2.3.4 Wavelet entropy

Wavelet Entropy (WE) is computed from the energy of each sub-band in the wavelet transform as written in (5) [17].

$$WE = -\sum_{i<0} p_i \ln p_i, \tag{5}$$

where p_i represents the wavelet relative energy obtained from (6).

$$p_i = \frac{E_i}{E_t} \ , \tag{6}$$

where E_i represents the energy for the i resolution, while E_t represents the total energy.

Noise can be eliminated when concentrated in the same frequency band, and changes can be detected in stationary signals based on the localization characteristic of wavelet transform [17]. Therefore, Db2 was employed as the mother wavelet with the seventh level of decomposition as conducted by Hashemi et al. [5].

2.3.5 Approximate entropy

Approximate Entropy (ApEN) is the feature of the signal complexity by calculating the number of occurrences of the signal pattern that occurred with the signal [18]. When the signal straddles along, hence:
$N\{u(i), 1 \le i \le N\}$, m is given to form the vector X_i^m up to X_{N-m+1}^m as in (7).

$$X_i^m = \{u(i),\ u(i+1),\ \ldots, u(i+m-1)\},\ i=1, \ldots,\ N-m+1, \tag{7}$$

where m represents the length of the window to be compared. For $i =\le N-m+1$, defined $C_i^m(r)$ is $(N-m+1)^{-1}$ multiplied by the sum of X_j^m in r from X_i^m. By defining $\varnothing^m(r)$ as in (8).

$$\varnothing^m(r) = (N-m+1)^{-1} \sum_{i=1}^{N-m+1} \ln C_i^m(r), \tag{8}$$

where ln represents natural logarithm, Pincus represents the ApEN as in (9) [18]:

$$ApEn(m,r) = \lim_{N \to \infty} \left[\Phi^m(r) - \Phi^{m+1}(r) \right]. \tag{9}$$

ApEN is estimated with the statistic, and then the ApEN becomes (10).

$$ApEn(m,r,N) = \Phi^m(r) - \Phi^{m+1}(r). \tag{10}$$

2.3.6 Sample entropy

Sample Entropy (SampEN) is an effort to overcome the disadvantages of ApEN proposed by Richman and Moorman [19]. In ApEN, there is a bias that occurs given self-matches where the code template of the signal is considered the same. SampEN is the measurement of the probability of the data series m that will be the same as another series in the signal with the tolerance of r, which will remain equal when the m data series increases to $m+1$. Equality refers to comparing the scalar distances between two vectors [18]. Mathematically, SampEN is shown in (11).

$$SampEN(m,r) = \lim_{N \to \infty} \left(-\ln \frac{A^m(r)}{B^m(r)} \right), \tag{11}$$

where $A^m(r)$ represents the probability in which the two series will be appropriate for $m+1$ in the tolerance r, and $B^m(r)$ represents the probability that the two series will be suitable for the number of m points in the tolerance r. In (11), self-matches are avoided. Furthermore, (11) can be estimated by creating

$$B = \{[(N - m - 1)(N - m)] / 2\}B^m(r),$$

$$A = \{[(N - m - 1)(N - m)] / 2\}A^m(r).$$

SampEN can be shown as in (12),

$$SampEN(m, r, N) = -\ln A/B. \tag{12}$$

The advantages of SampEN include being able to be used for short data series containing noise, distinguishing the wide variety of systems, performing better than ApEN based on the theory, and the consistency of entropy values for different pattern lengths uncalculated self-matches. Meanwhile, the disadvantages of SampEN are associated with the inconsistency of the entropy value for short data [20].

2.3.7 Permutation Entropy

Permutation Entropy (PE) calculates signal complexity by identifying the code between the sequences of the signals [21]. It analyzes the patterns of disparate elements in the signal and is shown in (13).

$$PE = -\sum_{j=1}^{n} p_j \log_2 p_j, \tag{13}$$

where p_j represents the relative frequency of the pattern of series. Meanwhile, n represents the permutation order with $n \geq 2$, and $n = 6$ was used according to Aziz and Arif [22].

2.3.8 Tsalli's Entropy

Tsalli's Entropy (TE) is commonly used to represent a system's physical behavior [23]. For example, it is described as a system with long-term memory effects, long-range interaction, and multifractal space-time constrain [24]. Furthermore, TE is not exhaustive, which means that when two identical systems exist, the total entropy is less than the sum of the two entropies. It is shown as in (14).

$$TE = \frac{1 - \sum_{i=1}^{W} p_i^q}{q - 1}, \tag{14}$$

where q is the measurement of non-extensity, p_i represents the discrete probability, and W is the microscopic configuration. TE can calculate any unexpected signal changes and show the effect of long-term memory on the signal strings. It has several advantages, including quantifying uncertainty, suitability for non-Gaussian calculations, and provision of more detailed information than ShEN.

2.4 Feature reduction

Feature reduction is intended to decrease the number of features used in the classification process. This is conducted by reducing the number of sub-bands used in the feature extraction process. The least number of features with the highest accuracy will be the recommendation of the method. In this study, methods such as feature subset selection were not used for feature reduction.

In the DWT method, because the 7th level of decomposition was used, then 8 sub-bands were obtained. Entropies were calculated in each sub-band as the features of the signal complexity. The sub-bands formed occupied the frequency as shown in **Table 2**. The feature reduction process omitted sub-bands A7, D2, and D1 because they did not provide the necessary information [4].

In the WPD, the 5th level of decomposition was used with the scenario, as shown in **Table 3,** to produce 15 sub-bands. First, feature reduction was made by eliminating the sub-bands occupying the frequency above 1000 Hz. The 8 sub-bands with a width of 125 Hz were then used [6].

2.5 Classifier

Multilayer Perceptron (MLP) is one of the architectures of neural networks that are often used to solve classification problems [25]. It is the simplest form of neural network architecture. It comprises three layers, i.e., the input, hidden, and output, as shown in Fig. 6.
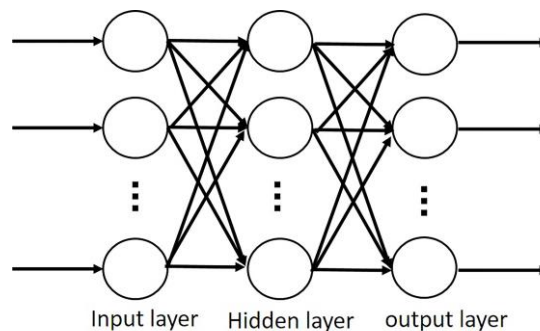

Fig. 6 – *Basic Configuration of MLP.*

A neuron-based input layer has as many attributes as recognized by the neurons. In contrast, an output layer contains as many classifications as acknowledged. The amount of neurons in the hidden layer is determined by trial and error [25]. MLP can be described through a one-neuron model such as in (15).

$$z = x_0 w_0 + x_1 w_1 + \cdots + x_n w_n = \sum_j x_j w_j, \tag{15}$$

where x represents the input signal and w is the weighting representing the synaptic modulation and determining how tough the input signal influences the neurotransmitter. Additionally, z represents the number of responses that affect the neurons.

The neuron's output is stated by the activation of function with the input of the total weighted response of the signal as represented by $y = f(z)$. The simplest function of y is the linear function, i.e., $y = z$. The sigmoid function is frequently used as an activation function in (16).

$$y = \frac{1}{1 + e^{-z}}. \tag{16}$$

In MLP, the back-calculation is conducted for the training process to change the value of w. The method used, for example, is backpropagation. In this study, MLP was only used to test the performance of the signal complexity of the multi-scale analysis method. However, it was not the focus of the discussion. This used MLP, a simple artificial neural network (ANN), not a deep learning method. MLP was selected because the other studies on lung sound classification also used the same method, making it easier to compare previous results using Hjorth descriptor on wavelet sub-band and MLP as classifier [26].

MLP network training necessitates data because it is part of supervised learning. N-Fold Cross Validation is a method for separating training from test data (NFCV). The N-1 dataset is utilized for training, whereas the other dataset is used for testing. Furthermore, each of the datasets is turned into test data, and the advantage of NFCV is regarding the accuracy value, which is relatively stable compared with the random distribution of test and training data [25].

This paper used 3fold CV to divide the lung data into three datasets. The first was used as testing data at the first iteration, while the remaining two were used as training data. The second dataset was also used as testing data in the iteration. In contrast, the other two were used as training data, and this process was repeated until the third iteration, as shown in Fig. 7. The advantage of a 3fold CV is that it reduces the possibility of overfitting. Therefore, only total accuracy was shown in the results of this study.
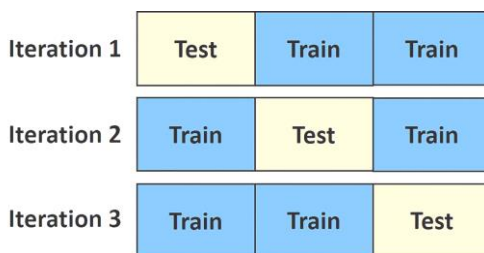
Fig. 7 – *Three-fold Cross-Validation.*

## 3   Result and Discussion

3.1 DWT entropy

Table 2 represents the result of DWT with 8 sub-bands. Furthermore, the number was reduced to 5 from D3 to D7, according to Kandaswamy et al. [4]. The classification was carried out using MLP and Three-Fold CV. The test for the 8 and 5 sub-bands are represented in **Table 4**.

Table 4 represents that DWT PE obtained the highest accuracy with 97.98% for Bior2.8 and Db8. DWT RE and DWT SEN also obtained an accuracy of 97.98% for Db8 and Db2. Reducing the number of sub-bands lowered the result of the accuracy.

Table 4
Accuracy (%) of DWT-Entropy.

Entropy	8 Sub-bands					5 Sub-bands				
	Bior2.8	Bior1.5	Db8	Db2	Haar	Bior2.8	Bior1.5	Db8	Db2	Haar
ShEN	90,91	86,87	87,88	88,89	86,87	77,78	66,67	82,83	75,76	72,73
RE	95,96	93,94	97,98	95,96	90,91	92,93	94,95	94,95	95,96	90,91
SEN	87,88	95,96	93,94	97,98	92,93	85,86	86,87	86,87	86,87	82,83
WE	75,76	79,8	85,86	87,88	87,88	71,72	73,74	76,77	76,77	76,77
TE	96,97	95,96	96,97	96,97	96,97	90,91	90,91	93,94	92,93	91,92
PE	97,98	93,94	97,98	94,95	92,93	90,91	81,82	95,96	93,94	81,82
SamEN	62,63	77,74	71,72	78,79	59,6	62,63	71,72	66,67	61,62	47,48
ApEN	87,88	89,9	92,93	90,91	86,87	84,85	77,78	83,84	78,79	77,78

As shown in **Table 4**, the best accuracy attained with five sub-bands was 95.96 % for DWT PE and DWT RE utilizing Db8 and Db2 as filters. This demonstrated that, despite the low energy in the sub-bands A7, D2, and D1, they contributed to the accuracy. The average PE and RE values for each sub-bands using the Db8 filter are shown in Fig. 8.
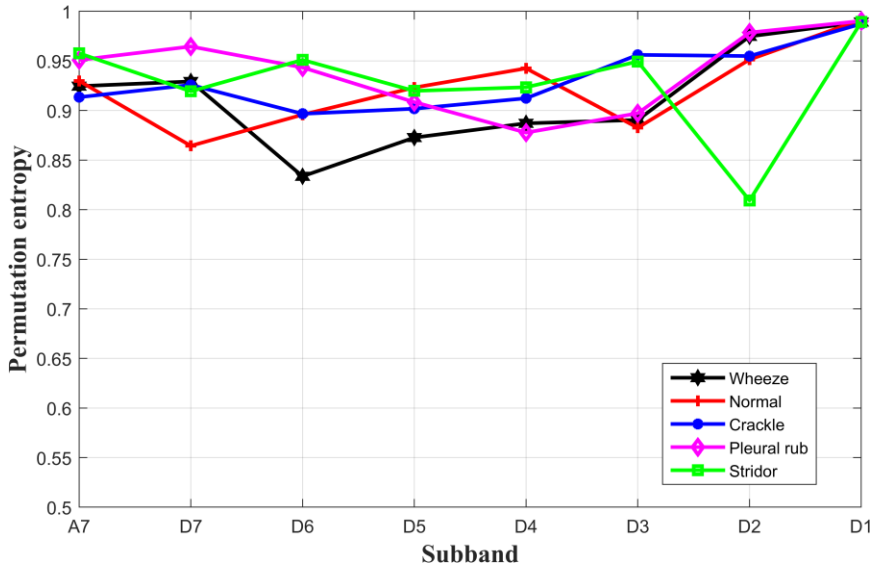
(a)
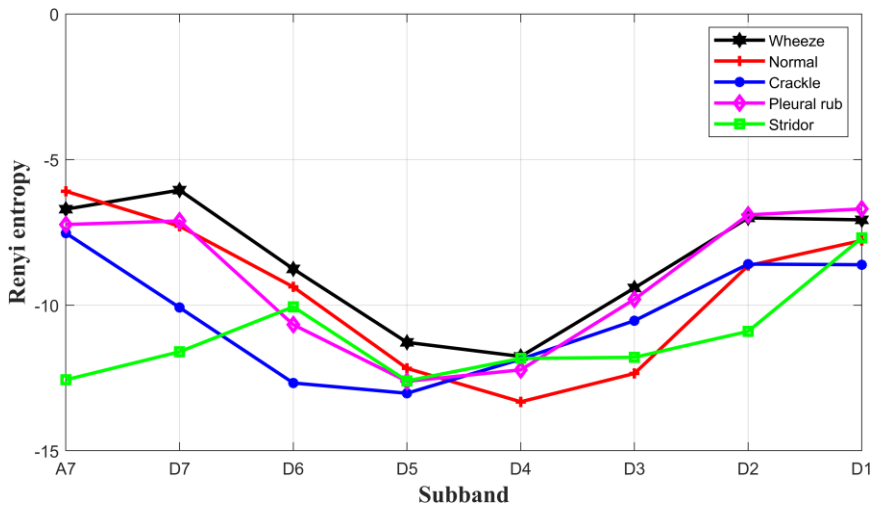
(b)

Fig. 8 − (a) *DWT-Permutation Entropy with Db8 Filter;*
(b) *DWT Renyi Entropy with Db8 Filter.*

As illustrated in Fig. 8 the PE value is relatively low (1) for all sub-bands. This corresponds with the PE formula and the permutation of the series of signals. Meanwhile, in Fig. 7b, the RE value is relatively large, with the negative value influenced by the RE used, i.e., 2nd order. The RE values are entirely separate between the classes in the sub-bands, D1, D2, and A7. This indicates when the three sub-bands are removed, the accuracy will be decreased. Meanwhile, there are no visible differences between classes in the sub-bands D1, D2, and A7 in the PE calculation. It is determined by the small differences in PE values between the sub-bands and classes. The minimum and maximum PE values are 0.809 and 0.992, respectively, with a standard deviation of 0.043. Even though the PE value is minimal, it is evident that the accuracy is relatively high.

Fig. 9 shows the comparison between crackle and friction rub features. The crackle data that were incorrectly identified are identical to those in the previous procedure. The fault is caused by the signal spectrum similar to the friction rub, resulting in the same entropy value for each sub-band.
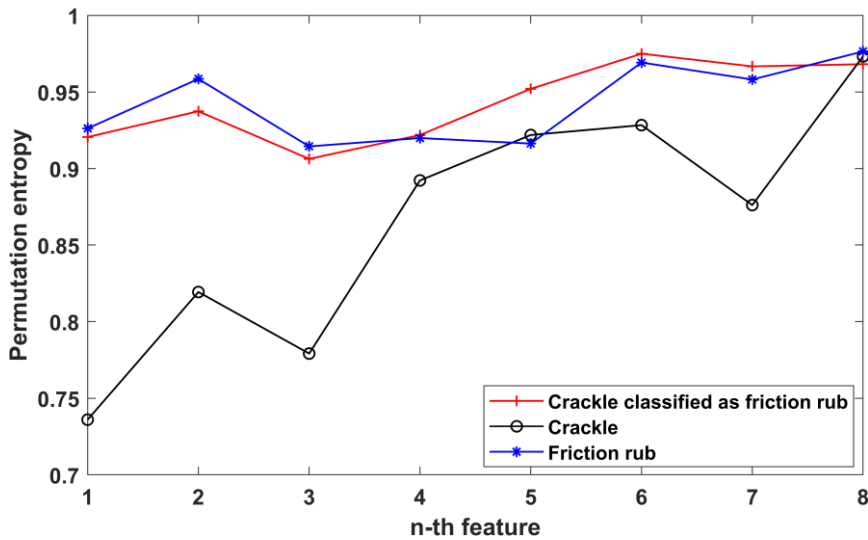

Fig. 9 – *Differences Between Crackle and Friction Rub Features.*

Generally, the lung sound frequency spectrum ranges from 50-1000 Hz [4]. Based on this information and range frequency of sub-band in Table 2, A7, D2, D1 range from 0-31.25 Hz, 1000-2000 Hz, and 2000-4000 Hz. Therefore, Figs. 1, 2, and 3 were visually confirmed, showing that the frequency spectrum >1000 Hz and < 50Hz is relatively low. However, in **Table 4**, eight sub-bands classification produced higher accuracy than five. It means that A7, D2, and D1 still significantly contribute to the classification accuracy.

3.2 WPD-Entropy

As illustrated in **Table 3**, WPD is a procedure that generates 15 sub-bands. Furthermore, the sub-bands will be reduced to 8, dividing the 0-1000 Hz frequency range into 125 Hz sub-bands [6]. The classification was carried out using MLP and NFCV. **Table 5** shows the test results for the 8 and 5 sub-bands.

Table 5

Accuracy (%) of WPD-Entropy

Entropy	15 sub-band				
	Bior2.8	Bior1.5	Db8	Db2	Haar
ShEN	93,94	91,92	97,98	92,93	89,9
RE	98,99	98,99	98,99	98,99	97,98
SE	93,94	94,95	94,95	93,94	92,93
WE	58,59	80,81	68,69	71,72	84,85
TE	86,87	93,94	90,91	87,88	92,93
PE	95,96	98,99	93,94	94,95	94,95
SamEN	97,98	97,98	95,96	97,98	94,95
ApEN	96,97	97,98	93,94	97,98	96,97
Entropy	8 sub-band				
	Bior2.8	Bior1.5	Db8	Db2	Haar
ShEN	89,9	92,93	87,88	92,93	90,91
RE	96,97	95,96	98,99	95,96	91,92
SE	86,85	96,97	76,77	84,85	92,93
WE	50,51	72,73	58,59	72,73	68,69
TE	90,91	93,94	94,95	92,93	91,92
PE	88,89	94,95	88,89	92,93	91,92
SamEN	96,97	96,97	97,98	97,98	94,95
ApEN	86,87	88,89	92,93	92,93	88,89

The highest accuracy with 98.99% for all wavelet filters except Haar was obtained for 15 sub-bands RE. Meanwhile, PE obtained 98.99% of the accuracy only for Bior1.5. Sub-bands reduction produced a similar accuracy for RE with the Db8 wavelet filter. Except for SampEN, which was steady, the lowering of sub-bands decreased accuracy, but SE and TE increased. The accuracy of SampEN remained constant due to the characteristic of SampEN, which

calculated the repetition of data patterns in the signal. The signal with high fluctuation was between 0 and 1000 Hz, and the significant SampEN value was located at this frequency. Meanwhile, SE and TE obtained increasing accuracy as the values of both at frequency >1000 Hz, which was relatively small and coincided between data classes. The accuracy is increased when the value is omitted.

As shown in **Table 5**, the accuracy of SampEN, SE, and ShEN was higher than DWT for 15 sub-bands. This showed that the decomposition scenario obtained the right sub-bands, and it distinguished each of the data classes very well. The low accuracy was obtained for DWT-entropy and WPD-entropy. The wavelet decomposition was performed twice on the signal using DWT or WPD and on the entropy using DWT. As a result, the information components in each sub-band are divided. This study used the 7th level of DWT with Db2, meaning that the possible decomposition and the wavelet filter did not match the needs.
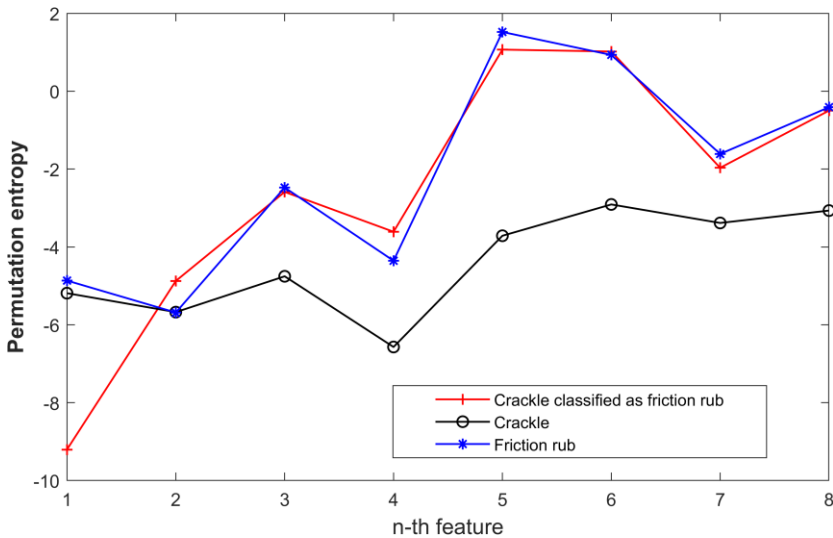

Fig. 10 – *Crackle and Friction Rub Features which Resulted in Error Classification.*

3.3 Discussion

Tables 4 and **5** show the analysis of various subjects, as seen below. At DWT level 7, feature reduction disregards the A7, D2, and D1 sub-bands, resulting in reduced accuracy. Despite having relatively limited information [14], the three frequency spectrum sub-bands were substantial enough to influence the classification procedure. The differences in DWT and WPD were caused by differences in width for the two processes. Meanwhile, 5 sub-bands on DWT and 8 on WPS occupy the same frequency range. Therefore, WPD generated 8 sub-bands with consistent widths, as seen in **Table 3**.

DWT produced different sub-band widths, as in **Table 2**. Therefore, the resulting features will also be different because the width sub-bands are different. With the sub-band width that is not uniform, the resulting DWT-entropy method sometimes cannot distinguish information at a 250-1000 Hz frequency, which is the difference in several types of lung sounds. Meanwhile, in WPD-entropy, the sub-band width is uniform at a frequency of <1000. This makes the feature reduction in WPD-entropy produce an accuracy as good as the 15 features in WPD-entropy.

Table 6 represents various comparative studies. The most similar method is the combination of WPD/DWT with the Hjorth descriptor [26]. The WPD/DWT Hjorth descriptor accuracy was 98.99% for 15 and 8 features. Meanwhile, DWT-entropy obtained the highest accuracy of 97.98%, while WPD-entropy obtained 98.99%. This showed that the proposed method obtained the same high accuracy as before.

Table 6
Comparison with the Previous Studies.

Ref.	*Dataset*	Method	Classifier	Number of Features	The Highest Accuracy
[27]	81 lung sound data, 5 classes	MLSD, Hjorth descriptor	MLP	20	97.98%
[14]	99 lung sound data, 5 classes	DWT level 7/WPD level 5, mean absolute value, mean average power, standard deviation of coefficient dan ratio of the mean absolute value of adjacent sub-band, skewness, kurtosis	MLP	46	97.98%/97.98%
[28]	85 data (normal, crackle, wheeze)	Higuchi FD, Katz FD, Entropy, Zero crossing, flux, roll-off, energy, kurtosis	KNN, SVM, Naïve Bayes	15	F-measure = 94.1%
[26]	99 lung sound data, 5 classes	DWT/WPD, Hjorth descriptor	MLP	24/8	98.99%
This Study	**99 lung sound data, 5 classes**	**DWT/WPD, entropy**	**MLP**	**8/8**	**97.98%/98.99%**

Principal component analysis (PCA) was not employed to reduce lung sound signal data in this investigation. PCA is a technique for data reduction while maintaining data variability. The weakness is losing information from the original data [29]. The difference between PCA and the proposed method is calculating the lung sound signal in the wavelet subband. The proposed hypothesis is based on the fact that each data class has a different frequency spectrum. Therefore, calculating the entropy in the signal decomposed subband is expected to distinguish the class of lung sounds. This study also used MLP instead of other classifiers. The usage makes the feature extraction method more visible, depending on the classifier. In addition, the use of MLP facilitates the comparison with previous studies using wavelets and MLP [14, 26].

The main contribution of this study is to provide an alternative feature extraction method for lung sound classification. Previously published study employed the average energy from the sub-band, the average sub-band coefficient's absolute value, the sub-band coefficient's standard deviation, and the absolute value ratio of each adjacent sub-band utilizing DWT at a sampling rate of 11,050 Hz [4]. In other studies, the energy was used in the WPD sub-band [6] and the Hjorth descriptor [26]. The feature proposed to be used is entropy in this study. Signal complexity from lung sounds can differentiate each type using entropy. With the entropy method, the number of features produced will be less with similar accuracy (98.99% using RE on the WPD).

The advantage is related to the ease in determining the sub-band selection scenario from the lung sound signal used. The entropy to be used can be chosen and changed to meet specific requirements. At the same time, the disadvantage of the proposed method is the absence of standard criteria for the sub-band selection. The selection method of an appropriate wavelet sub-band to improve the classification accuracy should be discussed in future studies.

4   Conclusion

The classification of lung sounds using wavelet decomposition and entropy was described. Five classes of normal bronchial, crackle, wheeze, pleural rub, and stridor data were used as the input data. First, wavelet decomposition was carried out using DWT and WPD with the decomposition scenario described previously. Furthermore, the results data were obtained by the entropy approach, and the feature reduction with classifier processes was conducted using Multilayer Perception (MLP). In the DWT process, the highest accuracy was obtained by DWT PE with an accuracy of 97.98% for Bior2.8 and Db8. DWT RE and DWT SEN also obtained an accuracy of 97.98% for Db8 and Db2. The WPD process obtained 15 sub-bands reduced to 8 to divide the 0-1000 Hz frequency into 125 Hz. The best results were given by RE using Db8 with 8 sub-bands, having an accuracy of 98.99%. Compared with the previous studies, the proposed method provides relatively high accuracy.

References

[1] P. P. Tanaka, M. Tanaka, D. R. Drover: Detection of Respiratory Compromise by Acoustic Monitoring, Capnography, and Brain Function Monitoring During Monitored Anesthesia Care, Journal of Clinical Monitoring and Computing, Vol. 28, No. 6, December 2014, pp. 561−566.

[2] A. Rizal, R. Hidayat, H. A. Nugroho: Comparison of Multilevel Wavelet Packet Entropy Using Various Entropy Measurement for Lung Sound Classification, International Journal of Advanced Computer Science and Applications, Vol. 10, No. 2, February 2019, pp. 77−82.

[3] J. Chen, Y. Dou, Y. Li, J. Li: Application of Shannon Wavelet Entropy and Shannon Wavelet Packet Entropy in Analysis of Power System Transient Signals, Entropy, Vol. 18, No. 12, December 2016, pp. 437- 1−437-14.

[4] A. Kandaswamy, C. S. Kumar, Rm. Pl. Ramanathan, S. Jayaraman, N. Malmurugan: Neural Classification of Lung Sounds Using Wavelet Coefficients, Computers in Biology and Medicine, Vol. 34, No. 6, September 2004, pp. 523−537.

[5] A. Hashemi, H. Arabalibiek, K. Agin: Classification of Wheeze Sounds Using Wavelets and Neural Networks, Proceedings of the International Conference on Biomedical Engineering and Technology, Vol. 11, Kuala Lumpur, Malaysia, June 2011, pp. 127−131.

[6] A. Rizal, T. L. R. Mengko, A. B. Suksmono: Lung Sound Recognition Using Wavelet Packet Decomposition and ART2 (Adaptive Resonance Theory 2) Neural Network, Proceedings of the International Biomedical Engineering Day, Vol. 2, 2006, pp. 2−6.

[7] H. M. de Oliveira: Shannon and Renyi Entropy of Wavelets, International Journal of Mathematics and Computer Science, Vol. 10, No. 1, February 2015, pp. 13−26.

[8] The R.A.L.E Repository, Available at:
http://www.rale.ca/Repository.htm [Accessed: 22-Jul-2015].

[9] D. Arnall: Breath Sounds, Available at:
http://jan.ucc.nau.edu/~daa/heartlung/breathsounds/contents.html [Accessed: 01-May-2015].

[10] The Auscultation Assistant - Breath Sounds, Available at:
http://www.med.ucla.edu/wilkes/lungintro.htm [Accessed: 01-Jun-2015].

[11] A. Bohadana, G. Izbicki, S. S. Kraman: Fundamentals of Lung Auscultation, The New England Journal of Medicine, Vol. 370, No. 8, February 2014, pp. 744−751.

[12] S. Reichert, R. Gass, C. Brandt, E. Andrès: Analysis of Respiratory Sounds : State of the Art, Clinical Medicine Insights: Circulatory, Respiratory and Pulmonary Medicine, Vol. 2, May 2008, pp. 45−58.

[13] S. G. Mallat: A Theory for Multiresolution Signal Decomposition: The Wavelet Representation, IEEE Transactions on Pattern Analysis and Machine Intelligence, Vol. 11, No. 7, July 1989, pp. 674−693.

[14] A. Rizal, R. Hidayat, H. A. Nugroho: Comparison of Discrete Wavelet Transform and Wavelet Packet Decomposition for the Lung Sound Classification, Far East Journal of Electronics and Communications, Vol. 17, No. 5, October 2017, pp. 1065−1078.

[15] M. Sabeti, S. Katebi, R. Boostani: Entropy and Complexity Measures for EEG Signal Classification of Schizophrenic and Control Participants, Artificial Intelligence in Medicine, Vol. 47, No. 3, November 2009, pp. 263−274.

[16] A. Renyi: On Measures of Entropy and Information, Proceedings of the 4th Berkeley Symposium on Mathematical Statistics and Probability, Vol. 1, Berkeley, USA, June 1960, pp. 547−561.

[17] O. A. Rosso, S. Blanco, J. Yordanova, V. Kolev, A. Figliola, M. Schürmann, E. Ba ar: Wavelet Entropy: A New Tool for Analysis of Short Duration Brain Electrical Signals, Journal of Neuroscience Methods, Vol. 105, No. 1, January 2001, pp. 65 – 75.

[18] S. M. Pincus: Approximate Entropy as a Measure of System Complexity, Proceedings of the National Academy of Sciences of the United States of America, Vol. 88, No. 6, March 1991, pp. 2297 – 2301.

[19] J. S. Richman, J. R. Moorman: Physiological Time-Series Analysis Using Approximate Entropy and Sample Entropy, American Journal of Physiology. Heart and Circulatory Physiology, Vol. 278, No. 6, June 2000, pp. H2039 – H2049.

[20] A. Humeau - Heurtier: The Multiscale Entropy Algorithm and Its Variants: A Review, Entropy, Vol. 17, No. 5, May 2015, pp. 3110 – 3123.

[21] C. Bandt, B. Pompe: Permutation Entropy: A Natural Complexity Measure for Time Series, Physical Review Letters, Vol. 88, No. 17, April 2002, pp. 174102-1 – 174102-5.

[22] W. Aziz, M. Arif: Multiscale Permutation Entropy of Physiological Time Series, Proceedings of the IEEE 9th International Multitopic Conference (IEEE INMIC), Karachi, Pakistan, December 2005, pp. 1 – 6.

[23] C. Tsallis: Possible Generalization of Boltzman-Gibbs Statistics, Journal of Statistical Physics, Vol. 52, No. 1-2, July 1988, pp. 479 – 487.

[24] U. R. Acharya, H. Fujita, V. K. Sudarshan, S. Bhat, J. E. W. Koh: Application of Entropies for Automated Diagnosis of Epilepsy Using EEG Signals : A review, Knowledge-Based Systems, Vol. 88, November 2015, pp. 85 – 96.

[25] R. Palaniappan: Biological Signal Analysis, Ventus Publishing ApS, London, 2010.

[26] A. Rizal, R. Hidayat, H. Adi Nugroho: Lung Sound Classification Using Hjorth Descriptor Measurement on Wavelet Sub-bands, Journal of Information Processing Systems, Vol. 15, No. 5, October 2019, pp. 2 – 14.

[27] A. Rizal, R. Hidayat, H. A. Nugroho: Hjorth Descriptor Measurement on Multidistance Signal Level Difference for Lung Sound Classification, Journal of Telecommunication, Electronic and Computeer Engineering (JTEC), Vol. 9, No. 2, April 2017, pp. 23 – 27.

[28] S. Don: Random Subset Feature Selection and Classification of Lung Sound, Procedia Computer Science, Vol. 167, 2020, pp. 313 – 322.

[29] I. T. Jolliffe, J. Cadima: Principal Component Analysis: A Review and Recent Developments, Philosophical Transactions of the Royal Society A: Mathematical, Physical and Engineering Sciences, Vol. 374, No. 2065, April 2016, pp. 1 – 16.